International Journal of Thermophysics, Vol. 24, No. 5, September 2003 (© 2003)

Study of an Optical Device Used to Homogenize a Laser Beam. Application to Emissivity Measurements on Semitransparent Materials at High Temperature[1]

A. Delmas[2,3] and J. C. Li[4]

On an experimental apparatus designed to measure the directional spectral emissivity of semitransparent materials at high temperature (2000°C), a specific optical device (kaleidoscope) is mounted in order to homogenize the energy distribution of a CO_2 laser beam, which is used as a heating source. An objective of this work, for operating in the best conditions, is to obtain a uniform temperature of the tested sample. This study, based on Fourier optics, focuses on a square aperture kaleidoscope. A model was developed to simulate the energy distribution of the laser beam, at any transverse plane on the optical path. The final objective is to simulate the energy distribution on the sample surface to optimize the homogenization device taking into account the surface temperature gradient induced by the local energy distribution. To validate this model, quantitative comparisons of theoretical simulations and experimental thermal spots are performed.

KEY WORDS: diffraction; emissivity; Fourier optics; homogenization; interference; semi-transparent materials.

1. INTRODUCTION

A knowledge of emissivity for semitransparent materials (STM) at high temperature, forms the subject of increasing interest among thermal

[1] Paper presented at the Sixteenth European Conference on Thermophysical Properties, September 1–4, 2002, London, United Kingdom.

[2] CETHIL Equipe TIM, UMR 5008, INSA de Lyon Bâtiment S. Carnot, 20, Avenue Albert Einstein, 69621 Villeurbanne Cedex, France.

[3] To whom correspondence should be addressed. E-mail: delmas@genserver.insa-lyon.fr

[4] Institute of Applied Laser, Kunming University of Science and Technology, Xue Fu Road #253, Kunming City, Yunnan Province 650093, People's Republic of China.

0195-928X/03/0900-1427/0

engineers and material physicists motivated by a constant demand from industry. The application domain is wide: thermal protections for spatial vehicles, modelling of radiative transfer in melting glass, etc.

The emissivity concept for STM is complex because being a volumetric property, it depends not only on the medium thickness, but also on its internal and surface temperature fields. Consequently, measurements of the emissivity on this type of material involve a specific metrology, and special care to be exercised in the best conditions. Using the principle of overlapping multiple beams, numerous studies of devices that convert an original energy distribution of a laser beam into a fairly homogeneous distribution have been performed [1–5].

The homogenization apparatus that we selected and will study here, is mainly composed of a square-section kaleidoscope, made of four flat rectangular mirrors, associated with two convergent lens. For easy use of such a system, a previous study was carried out [5]. Conclusions of this preliminary work showed that in the image plane, the energy distribution, obtained through recombination, even showing local drastic variations, was quite uniform in the sense of a local average, which is the expected result. However, in some specific conditions these interferences may damage the expected energy uniformity and be of the opposite effect that is desired. Thus, more detailed work is needed in order to predict the interference's function on the final energy distribution.

In addition, in the previous study [5] the incident laser beam was assumed to be of the Gaussian type, and effects of the spatial filter due to the very small circular aperture at the entrance of the kaleidoscope were not taken into account. The main objective being a quantitative analysis of the energy distribution in any transverse plane, the previous model used to simulate this distribution needs to be improved in order to be more representative of experimental conditions encountered on the emissivity bench [6]. Complementary simulations have shown that it is possible to optimize the setup by suppressing the main interfringe.

In the present study, the real energy distribution of the original laser beam, as well as effects of the spatial filter are taken into account, leading to results of simulation more accurate and closer to experimental prints on thermal paper performed on the experimental bench [6].

2. DESCRIPTION AND PRINCIPLE OF THE OPTICAL DEVICE

The optical device under study is presented in Fig. 1, where parameters and systems of reference used for simulations are defined. The laser beam, after exiting the cavity, crosses a first convergent lens L_0 of focal length f_0. The function of the lens is to focus radiation on the S point that is the

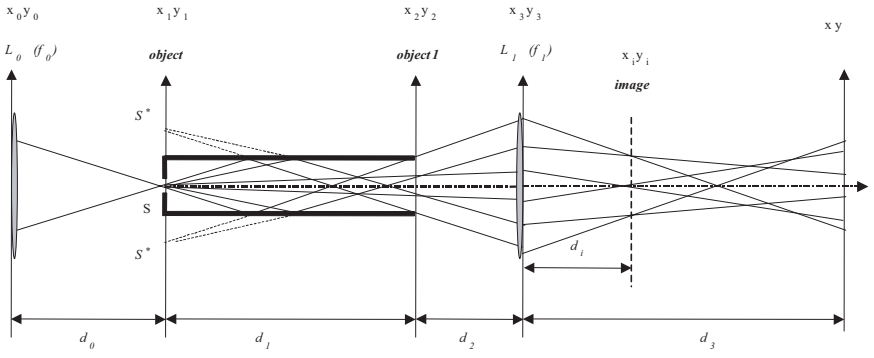

Fig. 1. Schematic of the optical setup and definitions of parameters.

center of the circular small aperture (1.14 ± 0.01 mm of diameter) placed at the center of the square entrance section of the kaleidoscope which is the next optical element of the system.

The kaleidoscope is composed of four rectangular plane mirrors forming a square section tube of $2L = 10$ mm sides, and a length of $d_1 = 200$ mm. Before exiting the kaleidoscope, beams go through multiple reflections on mirrors; this phenomenon, called the segmentation-recombination principle, is responsible for a quasi-homogeneous energy distribution. The beam then reaches a second convergent lens L_1 (focal length f_1). If the distance d_2 between the exit plane of the kaleidoscope referred to as object 1, and L_1, is greater than f_1, we obtain a real image of the exit square section. In object plane 1, the energy distribution of the beam can be considered as an overlapping of radiation coming from the real source S and its multiple images S^* through the flat mirrors. As a result of the superposition, we obtain a fairly uniform energy distribution in a local average.

The main objective of the present work is to analyze the energy distribution of the square spot at variable distance d_3 from L_1 (see Fig. 1).

3. SYSTEM ANALYSIS USING FOURIER OPTICS

Let $U_0(x_0, y_0) = \sqrt{P(x_0, y_0)}\exp(\frac{jk}{2R_0}(x_0^2 + y_0^2))$ be the complex amplitude of the spherical wave at a point with co-ordinates $(x_0, y_0, 0)$ before L_0. $P(x_0, y_0)$ is the power distribution, R_0 is the radius of the front wave, $k = \frac{2\pi}{\lambda}$, and $j = \sqrt{-1}$. If L_0 is considered to be a thin lens, its effect on the incident wave is only a phase transformation represented by the function $t_0(x_0, y_0)$. For paraxial theory, $t_0(x_0, y_0)$ can be written as

$$t_0(x_0, y_0) = \exp[jkn\Delta_0]\exp\left[-jk\frac{x_0^2 + y_0^2}{2f_0}\right] \quad (1)$$

In Eq. (1) the first term on the right-hand side, which is a function of both the relative refractive index n of the lens material, and of the thickness Δ_0, corresponds to a uniform phase difference. This term is irrelevant to our analysis of energy gradients and will not appear further in the complex field U.

Then, if r_0 is the radius of the pupil of L_0, the complex field U'_0 in a transverse plane directly after L_0 is linked to U_0 by the following relation:

$$U'_0(x_0, y_0) = T_0(x_0, y_0)\, U_0(x_0, y_0)$$

where

$$T_0(x_0, y_0) = \text{circ}\left(\frac{\sqrt{x_0^2+y_0^2}}{r_0}\right) \exp\left(-jk\,\frac{x_0^2+y_0^2}{2f_0}\right) \tag{2}$$

Let $U_1(x_1, y_1)$ be the complex amplitude in the entrance plane $x_1 y_1$ of the kaleidoscope located at d_0 from L_0. According to the theory of spatial frequency spectrum [7], U_1 can be expressed by

$$U_1(x_1, y_1) = \mathrm{F}^{-1}\{\mathrm{F}\{U'_0(x_0, y_0)\} \exp[jkd_0\sqrt{1-\alpha^2-\beta^2}]\} \tag{3}$$

where F and F^{-1} are, respectively, the Fourier transform and the inverse Fourier transform. α, β, and $\gamma = \sqrt{1-\alpha^2-\beta^2}$ are the direction cosines of the wave.

Taking into account only the presence of the entrance circular aperture of radius r_k, the complex amplitude in the exit plane $x_2 y_2$ is

$$U_2(x_2, y_2) = \mathrm{F}^{-1}\left\{\mathrm{F}\left\{U_1\left(x_1, y_1\right) \text{circ}\left(\frac{\sqrt{x_1^2+y_1^2}}{r_k}\right)\right\} \exp[jkd_1\sqrt{1-\alpha^2-\beta^2}]\right\} \tag{4}$$

Because of the multiple reflections on flat mirrors inside the kaleidoscope, the complex amplitude in the plane $x_2 y_2$ can be considered as the superposition of diffraction waves emanating from images S^* of the local sources S located at points with coordinates (x_m, y_m) in the entrance plane of the kaleidoscope.

$$\begin{cases} x_m = 2mL & m = \pm 1, \pm 2, \ldots \\ y_n = 2nL & n = \pm 1, \pm 2, \ldots \end{cases}$$

The complex amplitude of one of the images (subbeams) in the plane $x_2 y_2$ can be expressed as

$$U_{2mn}(x_2, y_2) = \text{rect}\left(\frac{x_2}{2L}\right)\text{rect}\left(\frac{y_2}{2L}\right) \times \rho^{|m|+|n|} U_2((-1)^{|m|}(x_2 - x_m), (-1)^{|n|}(y_2 - y_n)) \quad (5)$$

where $\text{rect}(\frac{x_2}{2L})\,\text{rect}(\frac{y_2}{2L})$ represents the transmittance in amplitude of the square exit aperture of the kaleidoscope. ρ $(0 < \rho < 1)$ is a parameter that can be used to account for the reflectivity of flat mirrors inside the kaleidoscope, for the specific wavelength of the CO_2 laser. ρ is assumed to be independent of direction in this first approach. $U_{3mn}(x_3, y_3)$ is the amplitude at a point of coordinates (x_3, y_3) immediately before L_1, using a similar expression to Eq. (3),

$$U_{3mn}(x_3, y_3) = \text{F}^{-1}\{\text{F}\{U_{2mn}(x_2, y_2)\} \exp[jkd_2\sqrt{1-\alpha^2-\beta^2}]\} \quad (6)$$

In a transverse plane just behind L_1, the complex amplitude U'_{3mn} is

$$U'_{3mn}(x_3, y_3) = \text{circ}\left(\frac{\sqrt{x_3^2+y_3^2}}{r_1}\right)\exp\left(-jk\frac{x_3^2+y_3^2}{2f_1}\right)U_{3mn}(x_3, y_3) \quad (7)$$

where r_1 is the radius of the pupil of L_1.

The expression for the complex amplitude $U_{mn}(x, y)$ in the observation plane xy, located at d_3 from L_1, is

$$U_{mn}(x, y) = \text{F}^{-1}\{\text{F}\{U'_{3mn}(x_3, y_3)\} \exp[jkd_3\sqrt{1-\alpha^2-\beta^2}]\} \quad (8)$$

Because each subbeam can be considered as a spherical wave, emanating from the source S or its images S^*, Eq. (8) can be written in the following form:

$$V_{mn}(x, y) = |U_{mn}(x, y)| \exp\left\{\frac{jk}{2(d_3 - d_i)}[(x - x_{mi})^2 + (y - y_{ni})^2]\right\}$$

$$\text{with} \quad \begin{cases} x_{mi} = M_i m \times 2L & (m = 0, \pm 1, \pm 2, \ldots, N) \\ y_{ni} = M_i n \times 2L & (n = 0, \pm 1, \pm 2, \ldots, N) \end{cases} \quad (9)$$

$M_i = -\frac{d_i}{d_1 + d_2}$ is the transverse enlargement in the image plane $x_i y_i$.

Considering that subbeams are perfectly coherent, we obtain a global complex amplitude by separate summation,

$$U(x, y) = \sum_{n=-N}^{N} \sum_{m=-N}^{N} V_{mn}(x, y)$$

Finally, we obtain the energy distribution in the observation plane as

$$I(x, y) = \sum_{m=-N}^{N} \sum_{n=-N}^{N} V_{mn}(x, y) \sum_{p=-N}^{N} \sum_{q=-N}^{N} V_{pq}^{*}(x, y) \tag{10}$$

Using Eq. (9) in the previous expression, the energy distribution is

$$I(x, y) = \sum_{m=-N}^{N} \sum_{n=-N}^{N} \sum_{p=-N}^{N} \sum_{q=-N}^{N} |U_{mn}(x, y)|\,|U_{pq}(x, y)| \times \cos\left[\frac{2\pi}{T_{mp}}\left(x - \frac{x_{mi} + x_{pi}}{2}\right)\right] \cos\left[\frac{2\pi}{T_{nq}}\left(y - \frac{y_{ni} + y_{qi}}{2}\right)\right] \tag{11}$$

with

$$T_{mp} = \frac{d_3 - d_i}{x_{pi} - x_{mi}}\,\lambda \tag{11a}$$

$$T_{nq} = \frac{d_3 - d_i}{y_{qi} - y_{ni}}\,\lambda \tag{11b}$$

Introducing a coherence factor F_{mnpq} [8] between subbeams that will be determined by experiments, using thermal spots, the distribution of absorbed energy in the plane xy for a time interval Δt is then expressed as

$$E(x, y) = \Delta t \sum_{m=-N}^{N} \sum_{n=-N}^{N} \sum_{p=-N}^{N} \sum_{q=-N}^{N} F_{mnpq}\,|U_{mn}(x, y)|\,|U_{pq}(x, y)| \times \cos\left[\frac{2\pi}{T_{mp}}\left(x - \frac{x_{mi} + x_{pi}}{2}\right)\right] \cos\left[\frac{2\pi}{T_{nq}}\left(y - \frac{y_{ni} + y_{qi}}{2}\right)\right]$$

$$\text{with} \quad F_{mnpq} = \begin{cases} 1 & (m = p \text{ and } n = q) \\ F_{\text{ch}} (0 < F_{\text{ch}} < 1) & (m \neq p \text{ or } n \neq q) \end{cases} \tag{12}$$

4. COMPARISON BETWEEN THEORETICAL AND EXPERIMENTAL RESULTS

The objective is to simulate the energy distribution in any transverse plane according to the approach previously described, and to make comparisons with impacts of the beam on thermal paper. Therefore, to carry out simulations, representative of experimental conditions presented in Fig. 2, we first need to characterize the original incident laser beam, and then to determine correlation coefficients introduced in Eq. (12).

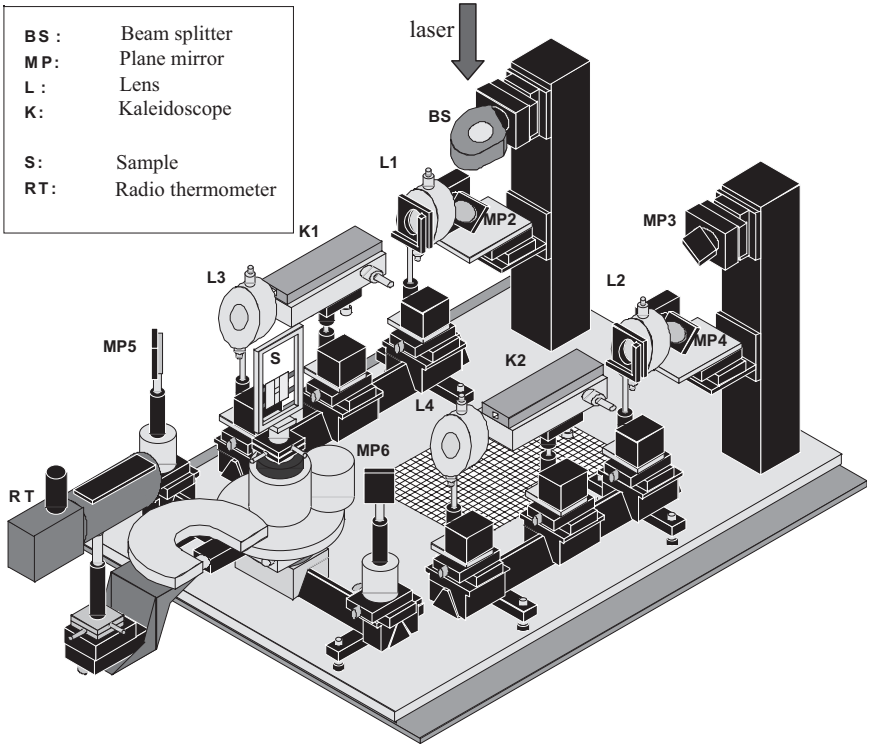

Fig. 2. Experimental apparatus to measure directional spectral emissivity of STM.

Tests are performed with a CO_2 laser source of wavelength $\lambda = 10.6$ μm in a continuous mode under an energy power $P_0 = 400$ W. A first impact of the incident beam, obtained on thermal paper placed directly at the exit of the cavity before the beam splitter (see Fig. 2), is presented in Fig. 3a.

Taking into account that the maximum of energy is not located at the center of the beam, the energy power in a transverse plane $x_0 y_0$ can be expressed as

$$P(x_0, y_0) = \frac{4P_0}{\pi w^2(2\eta+1)}\left[\eta \exp\left(-2\frac{(x_0-\Delta x)^2+(y_0-\Delta y^2)}{w^2}\right) + \frac{x_0^2+y_0^2}{w^2}\exp\left(-2\frac{x_0^2+y_0^2}{w^2}\right)\right] \quad (13)$$

In Eq. (13), η and w are parameters that can be used to simulate an energy distribution corresponding to the superposition of the two modes TEM00

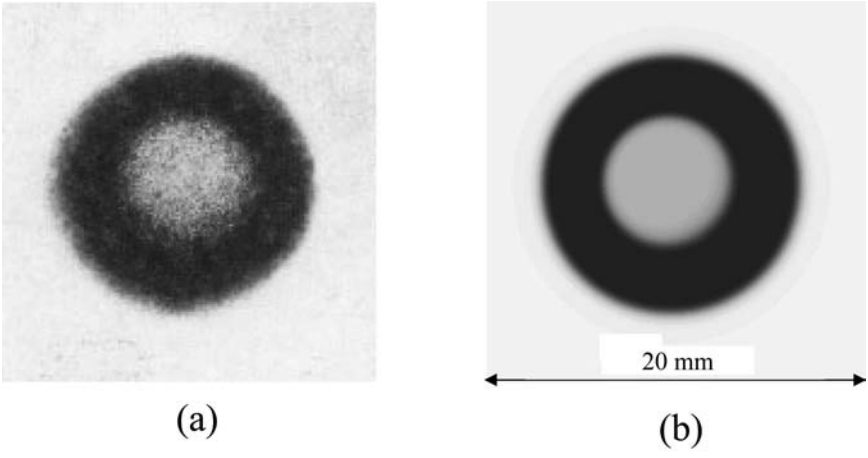

Fig. 3. Comparison between (a) prints on thermal paper and (b) simulation of energy distribution of the original laser beam.

and TEM01. $\eta = 0$ simulates the TEM01 mode of radius w; $\eta = \propto$ simulates the TEM00 mode of radius w. The following parameters Δx, Δy, w, and η are evaluated from the thermal print in Fig. 3a, and the corresponding simulation is presented in Fig. 3b.

In order to estimate N, which is the number of images to take into account, the diameter of the beam is considered to be $D = 6w$. According to geometrical relations illustrated by a simplified scheme in Fig. 4, if radiation issued from the Nth image is present at the square aperture exit of the kaleidoscope, we have

$$\Delta = \frac{Dd_1}{2d_0} - (2N-1)\,L > 0 \qquad \text{or} \qquad N < \frac{Dd_1}{4Ld_0} + \frac{1}{2}$$

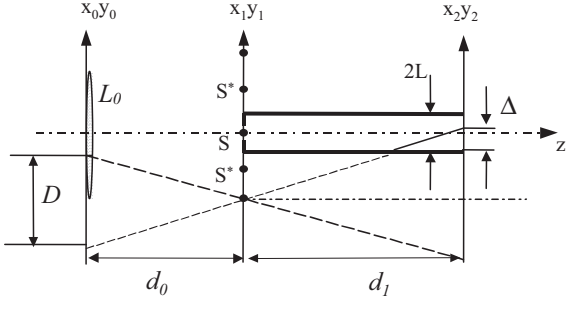

Fig. 4. Geometrical relations of images formed by the kaleidoscope.

Consequently, N is the integer part of the term on the right-hand side of the above inequality. To evaluate the energy loss through the system, we performed radiative flux measurements at the entrance, and behind optical elements. Results show that the total loss is close to 30%, with 10% between the cavity exit and the Kaleidoscope entrance, the last 20% being between the kaleidoscope entrance and the position of the image plane of L_1.

To simplify the energy loss study, we analyzed a thermal impact obtained near the image plane $x_i y_i$ reported in Fig. 5a. It can be seen that the heat flux decreases as the distance between the subbeam and the optical axis increases. In addition, the ρ factor introduced in Eq. (4) must satisfy the following condition:

$$\frac{\int_{-\infty}^{\infty}\int_{-\infty}^{\infty} U_1(x_1, y_1)\, U_1^*(x_1, y_1)\, \mathrm{d}x_1\, \mathrm{d}y_1 - \int_{-\infty}^{\infty}\int_{-\infty}^{\infty} U(x, y)\, U^*(x, y)\, \mathrm{d}x\, \mathrm{d}y}{\int_{-\infty}^{\infty}\int_{-\infty}^{\infty} U_1(x_1, y_1)\, U_1^*(x_1, y_1)\, \mathrm{d}x_1\, \mathrm{d}y_1} = 20\% \tag{14}$$

Equation (14) that leads to identify ρ can be solved provided that the correlation coefficient F_{ch} is known. We must point out that variations of this coefficient will only induce variations of contrast between interference fringes.

Equation (14) solved with $F_{\mathrm{ch}} = 0.4$ leads to a value of 0.82 for ρ that corresponds to a theoretical loss of 20.2%. This value providing a result in terms of energy loss, which is close to our measurements, is then used for the next simulations. In Fig. 5b is presented the simulation corresponding to the previous thermal spot (Fig. 5a).

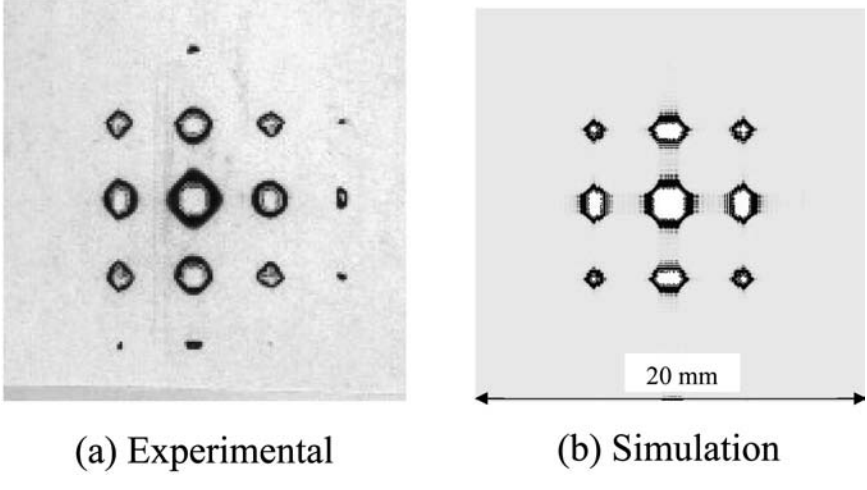

Fig. 5. Comparison between (a) prints on thermal paper and (b) simulation to determine ρ.

Table I. Experimental Parameters

P_0	w	R_0	f_0	f_1	d_0	d_1	d_2	Δt
400 W	5.2 mm	5000 mm	127 mm	127 mm	127 mm	200 mm	254 mm	10 ms

Simulation results can be presented in the form of numerical values, three-dimensional curves, or thermal impacts having the same color thresholds as that of the thermal paper used for experiments. Results are presented here through thermal impacts in order to establish a direct comparison with experiments. Parameters used for simulations are reported in Table I.

Figure 6 allows comparison between theoretical, and experimental thermal impacts obtained with the experimental setup (Fig. 2) for four values of d_3. The good agreement between predictions and measurements allows validation of the approach used for simulations.

It can be noticed that after going through the optical system, the energy distribution indicates both diffraction and interference fringes. In the image plane ($d_3 = d_2 = 254$ mm), interference fringes and an energy distribution fairly uniform on average inside the square spot with sharp edges can be observed.

We can also observe that only one group of interfringes can be seen, resulting from interferences between the S source on the axis and its closer image S^*. Theory can be used to predict correctly this phenomenon.

In Table II we present comparisons between fringe spacings predicted by simulations and measured results for thermal paper impacts.

Table II. Comparisons of Interfringes

d_3 (mm)	Theoretical interfringes (mm)	Experimental interfringes (mm)
114	0.170	0.17 ± 0.01
208	0.086	0.09 ± 0.01
228	0.141	0.14 ± 0.01
254	0.212	0.21 ± 0.01
276	0.272	0.27 ± 0.01

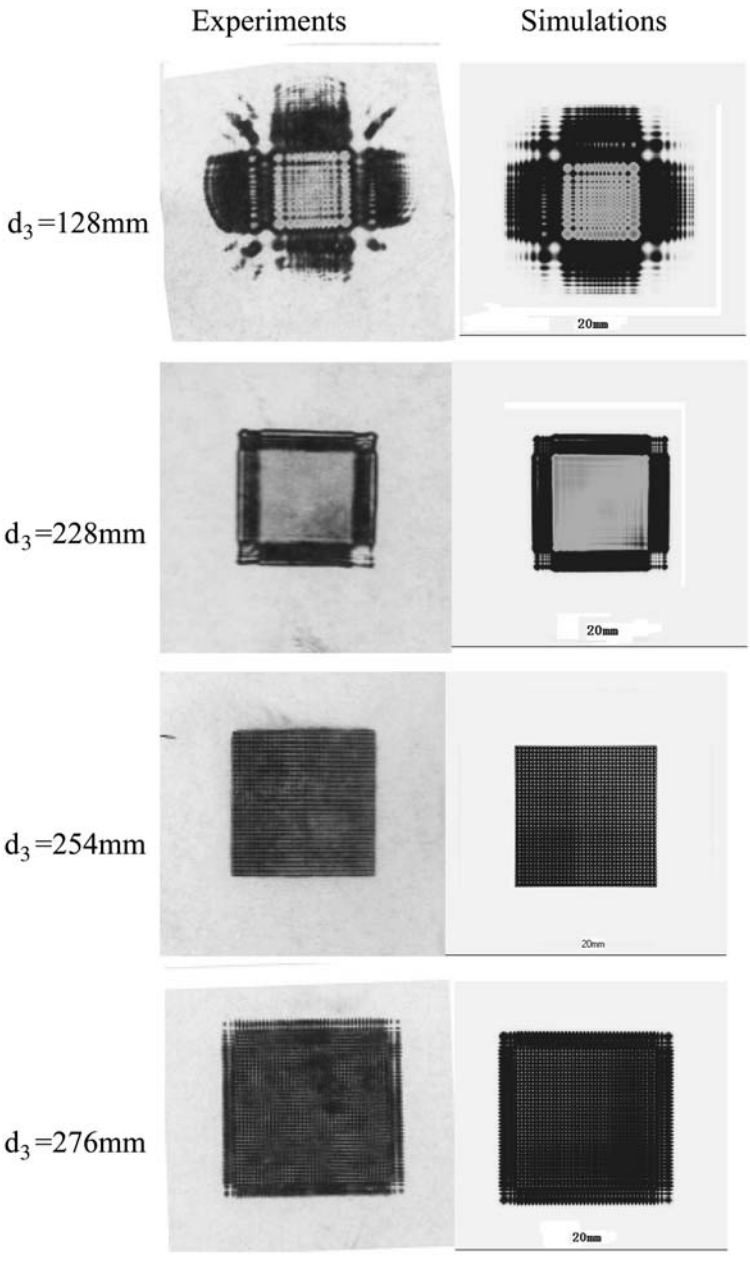

Fig. 6. Experimental and theoretical impacts for four values of d_3.

5. CONCLUSIONS AND PERSPECTIVES

Through a theoretical approach based on Fourier optics, we are able to simulate the energy distribution of the CO_2 laser beam after going through a homogenization device that includes a kaleidoscope. Comparison of impacts on thermal paper and simulations show good agreement between experiments and predictions; consequently, we are able to predict with good accuracy, the energy distribution of the beam, in any transverse plane; in particular, in the sample plane to be heated provided that the initial incident beam is perfectly characterized.

Then, the following applications of modelling of the homogenization system can be considered:

Firstly, it can be considered as a tool for optimization of the system, as well as for providing key help for the adjustment and alignment of the optical bench (Fig. 2). Secondly, associated with three dimensional (3D) modelling of coupled heat transfers by conduction and radiation in semitransparent materials (STM), a knowledge of the energy distribution will lead to predictions of the surface and inside temperature fields, provided that radiative properties of the tested material are known.

Modelling of coupling heat transfer mechanisms in STMs submitted to an incident radiative heat flux distribution is an important part of the metrology linked to determination of the emission factor at high temperature. Measurements of the emissivity on STMs are valid only under the requirement that the medium is either isothermal or if effects of a nonuniform temperature are negligible on the radiative heat flux leaving the sample. Studies on this particular point are currently being carried out. This work is an extension to semitransparent materials of studies on interactions between lasers and opaque materials [9].

Even if we presented here a specific application of the study of the optical device, an optimization of the CO_2 laser beam conditioning for heating ceramic samples at high temperature, there are lots of other applications for this study. In fact, as soon as the objective is to control the homogenization of any radiation or even its energy distribution after going through optical systems that present diffraction, a similar study is necessary.

Let us note that the present study concern monochromatic coherent radiation. One of the perspectives of this work is then to extend this approach to polychromatic radiation.

REFERENCES

1. Y. Kawamura, Y. Itagaki, K. Toyoda, and S. Namba, *Optics Comm.* **48**:44 (1983).
2. D. M. Dangenais, J. A. Woodroffe, and I. Itzkan, *Appl. Optics* **24**:67 (1985).

3. J. C. Li, J. Merlin, and J. Perez, *Rev. de Phys. Appl.* **21**:425 (1986).
4. G. Herziger and E. W. Kreutz, *SPIE* **1024**:2 (1988).
5. J. C. Li, R. Lopes, Ch. Vialle, and J. F. Sacadura, *J. Laser Appl.* **1**:279 (1999).
6. R. Lopes, A. Delmas, and J. F. Sacadura, *High Temp.-High Press.* **32**:369 (2000).
7. J. W. Goodman, *Introduction to Fourier Optics* (McGraw–Hill, New York, 1968).
8. J. C. Li, C. Vialle, and J. Merlin, *J. Opt.* **24**:41 (1993).
9. J. C. Li and J. Merlin, *J. Phys. III* **1**:331 (1991).

Printed in Belgium